Pergamon

Int. J. Heat Mass Transfer. Vol. 37, Suppl. 1, pp. 381–393, 1994

0017–9310/94 $6.00+0.00

0017–9310(93)E0047–K

Benchmark results in computational heat and fluid flow: the integral transform method

RENATO M. COTTA

Mechanical Engineering Department, EE/COPPE/UFRJ, Universidade Federal do Rio de Janeiro, Cx.Postal 68503, Cidade Universitária, Rio de Janeiro, RJ 21945 970, Brazil

Abstract—The integral transform method is reviewed as a benchmark tool in computational heat and fluid flow, with special emphasis on nonlinear problems. The hybrid numerical–analytical nature of this approach collapses the numerical task into one single independent variable, and thus allows for a simple computational procedure with automatic global error control and mild increase in computational effort for multidimensional situations. Various applications on nonlinear diffusion and convection–diffusion are more closely considered, followed by sample results from recent contributions.

INTRODUCTION

THE INTEGRAL transform method is well-known as a classical approach in the analytical solution of certain classes of linear transformable diffusion problems [1, 2]. The treatise by Mikhailov and Özisik [3] compiles most of the available work in the exact analysis of heat and mass diffusion, following the ideas of integral transformation. During the last two decades, after the work of Özisik and Murray [4], this approach was progressively extended to allow for the approximate analytical solution of a much wider range of a priori non-transformable problems, as reviewed in different sources [5–8].

More recently, this approach gained a hybrid numerical–analytical structure, offering user controlled accuracy and quite efficient computational performance for a wide variety of problems, which are classified and systematically presented with several applications in ref. [5], including the nonlinear formulations of interest in heat and fluid flow applications. Among the various types of extensions discussed in ref. [5], we can briefly point out problems with variable equation and boundary coefficients, moving boundary problems, irregular non-transformable geometries, difficult auxiliary eigenvalue-type problems, coupled problems, nonlinear diffusion and convection–diffusion problems, boundary layer formulations and Navier–Stokes equations.

Besides being an alternative computational method in itself, this revived approach is particularly well-suited for benchmarking purposes, in light of its automatic error control feature, retaining the same characteristics of a purely analytical solution. In addition to the straightforward error control and estimation, an outstanding aspect of the method is the direct extension to multidimensional situations, with a rather mild increase in computational effort with respect to one-dimensional applications. Again, the hybrid nature is responsible for this behavior, since the analytical part in the solution procedure is employed over all but one independent variable, and the numerical task is always reduced to the integration of an ordinary differential system in one single coordinate.

The nonlinear formulations in heat and fluid flow that have been handled, can be divided, for illustration purposes, into five different classes, namely, diffusion type-problems [9–17], convection–diffusion problems [17–20], eigenvalue problems [21], boundary layer equations [22–24], and Navier–Stokes equations [25–28].

The present paper reviews specifically such nonlinear problems of great practical interest, that have been tracted so far through the generalized integral transform technique and briefly indicates how the computational algorithm proceeds in this approach. A number of representative nonlinear examples are then examined more closely.

FORMAL SOLUTION

As an example of the formal solution procedure, let us consider the following transient nonliner diffusion problem, defined within region V and boundary surface S, with nonlinear source functions at both equation and boundary condition

$$w(\mathbf{x})\frac{\partial T(\mathbf{x},t)}{\partial t} = \nabla\cdot K(\mathbf{x})\nabla T(\mathbf{x},t) - d(\mathbf{x})T(\mathbf{x},t) + P(T(\mathbf{x},t)), \quad \text{in } \mathbf{x}\in V, \quad t>0 \tag{1a}$$

with boundary and initial conditions given respectively by

$$\alpha(\mathbf{x})T(\mathbf{x},t)+\beta(\mathbf{x})K(\mathbf{x})\frac{\partial T(\mathbf{x},t)}{\partial \mathbf{n}} = \phi(T(\mathbf{x},t)), \quad \mathbf{x}\in S, \quad t>0 \tag{1b}$$

$$T(\mathbf{x},t) = f(\mathbf{x}), \quad \mathbf{x}\in V, \quad t=0. \tag{1c}$$

NOMENCLATURE

$d(\mathbf{x})$	coefficient of L operator, equation (2b)
$f(\mathbf{x})$	initial condition (1c)
$\bar{f}_i$	transformed initial condition
$\bar{g}_i$	transformed source functions
$K(\mathbf{x})$	coefficient of L operator, equation (2b)
$\mathbf{n}$	outward drawn normal vector
N	order of truncated system
N_i	normalization integral
$P(T(\mathbf{x}, t))$	source function of equation (1a)
t	time or corresponding space coordinate
S	region boundary surface
$\bar{T}_i(t)$	transformed potential
$T(\mathbf{x}, t)$	potential
V	region volume
$w(\mathbf{x})$	coefficient of L_t operator, equation (2a)
$\mathbf{x}$	position vector.

Greek symbols

$\alpha(\mathbf{x})$	coefficient of boundary condition, equation (1b)
$\beta(\mathbf{x})$	coefficient of boundary condition, equation (1b)
ε	relative error estimator, equation (7)
μ_i	eigenvalues of problem (3)
$\phi(T(\mathbf{x}, t))$	source function in boundary condition (1b)
$\psi(\mu_i, \mathbf{x})$	eigenfunctions of problem (3).

Although the nonlinearities appear explicitly only in the source terms of both equation (1a) and boundary condition (1b), such a formulation includes more general ones, provided the linear operators

$$L_t \equiv w(\mathbf{x})\frac{\partial}{\partial t} \tag{2a}$$

$$L \equiv -\nabla\cdot K(\mathbf{x})\nabla + d(\mathbf{x}) \tag{2b}$$

$$B \equiv \alpha(\mathbf{x}) + \beta(\mathbf{x})K(\mathbf{x})\frac{\partial}{\partial \mathbf{n}} \tag{2c}$$

are taken as characteristic ones extracted from the original nonlinear versions, and remaining nonlinear terms are collapsed into the source functions, $P(T)$ and $\phi(T)$.

By following the formalism in the generalized integral transform technique, the auxiliary eigenvalue problem is taken as

$$\nabla\cdot K(\mathbf{x})\nabla\psi(\mu_i, \mathbf{x}) + (\mu_i^2 w(\mathbf{x}) - d(\mathbf{x}))\psi(\mu_i, \mathbf{x}) = 0, \quad \mathbf{x}\in V \tag{3a}$$

$$\alpha(\mathbf{x})\psi(\mu_i, \mathbf{x}) + \beta(\mathbf{x})K(\mathbf{x})\frac{\partial\psi_i(\mathbf{x})}{\partial \mathbf{n}} = 0, \quad \mathbf{x}\in S \tag{3b}$$

whose solution is assumed to be known at this point, and allows the definition of the following integral transform pair:

$$\bar{T}_i(t) = \int_V w(\mathbf{x})\frac{\psi_i(\mathbf{x})}{N_i^{1/2}} T(\mathbf{x}, t)\, dv, \quad \text{Transform} \tag{4a}$$

$$T(\mathbf{x}, t) = \sum_{i=1}^{\infty} \frac{1}{N_i^{1/2}}\psi_i(\mathbf{x})\bar{T}_i(t), \quad \text{Inversion.} \tag{4b}$$

Equation (1a) is now operated on with $\int_V \psi_i(\mathbf{x})/N_i^{1/2}\, dv$, to yield:

$$\frac{d\bar{T}_i(t)}{dt} + \mu_i^2\bar{T}_i(t) = \bar{g}_i(T) \tag{5a}$$

where,

$$\bar{g}_i(T) = \int_V \frac{\psi_i(\mathbf{x})}{N_i^{1/2}} P(T(\mathbf{x}, t))\, dv + \frac{1}{N_i^{1/2}}\int_S K(\mathbf{x}) \times \left[\psi_i(\mathbf{x})\frac{\partial T(\mathbf{x}, t)}{\partial \mathbf{n}} - T(\mathbf{x}, t)\frac{\partial\psi_i(\mathbf{x})}{\partial \mathbf{n}}\right] ds. \tag{5b}$$

The surface integral above is now evaluated by making use of boundary conditions (1b) and (3b), which after some manipulations yield:

$$\int_S K(\mathbf{x})\left[\psi_i(\mathbf{x})\frac{\partial T(\mathbf{x}, t)}{\partial \mathbf{n}} - T(\mathbf{x}, t)\frac{\partial\psi_i(\mathbf{x})}{\partial \mathbf{n}}\right] ds = \int_S \phi(T(\mathbf{x}, t))\left\{\frac{\psi_i(\mathbf{x}) - K(\mathbf{x})[\partial\psi_i(\mathbf{x})/\partial \mathbf{n}]}{\alpha(\mathbf{x}) + \beta(\mathbf{x})}\right\} ds. \tag{5c}$$

Also, the initial condition (1c) is transformed with $\int_V w(\mathbf{x})\psi_i(\mathbf{x})/N_i^{1/2}\, dv$, and the completely transformed problem is given by:

$$\frac{d\bar{T}_i(t)}{dt} + \mu_i^2\bar{T}_i(t) = \bar{g}_i(\bar{T}_j(t)), \quad j = 1, 2, \ldots \tag{6a}$$

$$\bar{T}_i(0) = \bar{f}_i, \quad i = 1, 2, \ldots \tag{6b}$$

where,

$$\bar{g}_i(\bar{T}_j) = \frac{1}{N_i^{1/2}}\left\{\int_V P(\mathbf{x}, \bar{T}_j(t))\psi_i(\mathbf{x})\, dv + \int_S \phi(\mathbf{x}, \bar{T}_j(t))\left[\frac{\psi_i(\mathbf{x}) - K(\mathbf{x})[\partial\psi_i(\mathbf{x})/\partial \mathbf{n}]}{\alpha(\mathbf{x}) + \beta(\mathbf{x})}\right] ds\right\} \tag{6c}$$

and,

$$\bar{f}_i = \frac{1}{N_i^{1/2}}\int_V w(\mathbf{x})f(\mathbf{x})\psi_i(\mathbf{x})\, dv. \tag{6d}$$

Equations (6) above form an infinite system of nonlinear ordinary differential equations for the transformed potentials, $\bar{T}_i$s. Once a solution is obtained, the inversion formula, equation (4b), can be recalled to provide the complete field, $T(\mathbf{x}, t)$. From an engin-

eering point of view it suffices to truncate the infinite system at the Nth row and column, solve this $N \times N$ system, and observe the convergence behavior as N is increased. From a more formal point of view, it is necessary to look for conditions on the right hand sides of equation (6a) ensuring that the solution tends to the solution of the infinite system as $N \to \infty$, as indicated in ref. [5]. For computational purposes, the truncation order N is adaptively chosen along the numerical integration process, so as to satisfy the user prescribed accuracy target and keeping the computational effort to a minimum. The aspects related to the adaptive computational procedure are discussed in the next section, including the automatic error control scheme.

Applications are then considered to illustrate the computational procedure and demonstrate the convergence behavior for each class of nonlinear problem here analyzed.

COMPUTATIONAL PROCEDURE

The basic steps in applying the generalized integral transform technique are as follows.

(A) Choose an appropriate auxiliary problem, which contains as much information as possible about the original problem, with respect to the geometry and operators in the coordinates to be eliminated through integral transformation. The more information contained in the expansion basis functions, the less coupled the resulting ordinary differential system will be and the smaller the number of terms required in the system truncation.

A number of eigenvalue problems are readily solved in explicit analytic form in terms of well-known transcendental functions, otherwise the integral transform approach itself can be used to provide a semi-analytic error controlled solution to the original auxiliary problem, as discussed in ref. [5].

(B) Develop the integral transform pair for the associated transformation and inversion operations, which is a straightforward task once the orthogonality property of the eigenfunctions has been obtained. For classical Sturm–Liouville problems these results are readily available, as well as for a number of more general situations [3].

(C) Integral transform the original partial differential system, by making use of the appropriate operator that recovers the transform formulae within the transformation process. The related integral operator will be responsible for eliminating all but one independent variable of the PDE system, but not every term will be fully transformable in the sense of ref. [3]. Therefore, an infinite system of nonlinear coupled ordinary differential equations will result, relating the infinitely many transformed potentials of the eigenfunctions expansion. If a decoupled system was obtained, each transformed potential could be independently solved and an exact solution would be achievable.

(D) Numerically solve the coupled ODE system, after truncation of the infinite system at the Nth row and column. The formal aspects behind this truncation process, which warrant convergence to the infinite system solution as N increases, were examined more closely in different sources [5]. The numerical procedures adopted are better discussed in this section, and involve the use of well-established ODE solvers available in scientific subroutines packages such as the IMSL library [29], with user prescribed accuracy. Note that for parabolic problems the ODE system becomes an initial value problem, while for elliptic systems a boundary value problem results. In the case of an eigenvalue problem, the integral transformation process produces an algebraic problem for the related matrix eigensystem analysis.

Under certain circumstances, approximate solutions may be of interest in the realm of applications, readily obtainable by neglecting the nondiagonal elements in the coupled ODE system, yielding a decoupled 'lowest order solution', or its once analytically iterated companion, the 'iterated lowest order solution'.

(E) Recall the inversion formula to construct the original potentials, once the transformed potentials have been numerically evaluated in the previous step. Therefore, the final solution is analytic and explicit in all but one of the independent variables, and the summations of the inversion formula are computed only at those points of interest, or analytically manipulated as needed. Thus, the truly numerical task in this approach is reduced to the error controlled solution of an ODE system.

A quite straightforward algorithm can be constructed, including the attractive feature of automatically controlling the global error in the final solution at any selected points. To achieve this goal, the semi-analytic nature of this approach is used in conjunction with well-established subroutines libraries with intensively tested accuracy control schemes. The basic steps in computation are as follows.

(A) The auxiliary eigenvalue problem is solved for the eigenvalues and related normalized eigenfunctions, either in analytic form when applicable or through the generalized integral transform technique itself.

(B) The transformed initial or boundary conditions are computed, either analytically or, in a general purpose procedure, through adaptive numerical integration, such as in subroutine DQDAGS from the IMSL package [29]. Similarly, those coefficients on the transformed ODE system which are not dependent on the transformed potentials can be evaluated a priori, and therefore saving some computational effort during the numerical integration of the ODE system.

(C) The truncated ODE system is then numerically

solved through different tools, depending on the type of problem under consideration. For an initial value problem, the numerical integration is performed, for instance, through subroutine DIVPAG of the IMSL library in Gear's method mode, since the resulting system is likely to become stiff, especially for increasing truncation orders. Boundary value problems can be handled through the subroutine DBVPFD, which is a more recent implementation of the well-known PASVA3 code, an adaptive finite-difference program for first order nonlinear boundary value problems. Both subroutines offer an interesting combination of accuracy control, simplicity in use and reliability, with some compromise in speed and memory requirements when compared to dedicated schemes. In either case, a pre-estimate for the truncation order N can be obtained, for instance, through the lowest order solution. Since all the intermediate numerical tasks are accomplished within user prescribed accuracy, one is left with the need of reaching convergence in the eigenfunction expansions and automatically controlling the truncation order N, for a certain number of fully converged digits requested in the final solution, at those positions of interest.

The analytic nature of the inversion formulae allows for a direct testing procedure at each specified position within the medium where a solution is desired, and the truncation order N can be gradually decreased (or eventually increased), to fit the user global error requirements over all the solution domain. The simple tolerance testing formula employed is written as:

$$\varepsilon = \max_{\mathbf{x}\in r} \left| \frac{\sum_{i=N^*}^{N} \frac{1}{N_i^{1/2}} \psi_i(\mathbf{x}) \bar{T}_i(t)}{\sum_{i=1}^{N} \frac{1}{N_i^{1/2}} \psi_i(\mathbf{x}) \bar{T}_i(t)} \right| \tag{7}$$

where N^* is decreased from the value of N while ε still fits the user requested global error, and then N is changed to assume the value of N^*. The truncation order can also be increased and numerical integration repeated in case the estimated value of N is not sufficiently large to provide the required number of fully converged digits.

For parabolic systems, i.e. initial value problems, in which numerical integration follows a marching procedure along the t variable, this adaptive scheme of controlling N automatically reduces the system size as integration proceeds in t. It is then recommended to start the marching procedure with a conservatively high value of N and allow the adaptive scheme to play the role of reducing and controlling N.

Significant computational savings are achieved with respect to a plain numerical integration with a fixed size system. For elliptic systems (boundary value problems), in which numerical integration is performed at once for all the solution domain, through an iterative procedure, there is no relative gain in repeating computations for a reduced system size, since a more precise solution is already available (except for the need of inspecting how accurate this solution might be). Therefore, it is recommended that integration is started with an underestimated value of N, and the truncation order can then be gradually increased in fixed steps, $N+\Delta N$, until convergence is achieved in all desired locations. The lower order results already available then serve as excellent initial guesses for the iterative procedure implemented in the boundary value problem solver, providing a faster solution of the higher order ODE system. In both cases, the adaptive scheme automatically controls the relative error on the final converged solution, and offers in addition a costless error estimator at completion of the integration.

APPLICATIONS

Nonlinear source term (diffusion problem) [9]

We consider the transient analysis of a radiating fin subjected to step changes in base or ambient temperture [9], with a nonlinear surface dissipation term, written in dimensionless form as:

$$\frac{\partial T(\mathbf{x},t)}{\partial t} = \frac{\partial^2 T(\mathbf{x},t)}{\partial \mathbf{x}^2} - N_c(T^4 - H^4), \quad \text{in } 0 < \mathbf{x} < 1, \quad t > 0 \tag{8a}$$

$$T(\mathbf{x},0) = T_0, \quad 0 \leqslant \mathbf{x} \leqslant 1 \tag{8b}$$

$$\left.\frac{\partial T(\mathbf{x},t)}{\partial x}\right|_{x=0} = 0; \quad T(1,t) = 1, \quad t > 0. \tag{8c,d}$$

In order to present some representative results, three cases were taken from the related literature, and an analysis of convergence was performed for increasing values of the order N and at different times t. All the numerical results reported were obtained by making use of subroutine DIVPAG from the IMSL package, with a relative error requirement of 10^{-5}.

The convergence rates can be observed by considering different orders of truncation, N, for the dimensionless temperature profile. Table 1 shows the convergence of the temperature profile at $t = 0.09$ and

Table 1. Radiating fin analysis: convergence of temperature profile ($t = 0.09$)

x	$N = 5$	$N = 10$	$N = 15$	$N = 20$ or 30
0.0	0.5145	0.5146	0.5146	0.5146
0.1	0.5178	0.5178	0.5178	0.5178
0.2	0.5280	0.5279	0.5279	0.5279
0.3	0.5459	0.5459	0.5459	0.5459
0.4	0.5737	0.5739	0.5738	0.5738
0.5	0.6134	0.6133	0.6133	0.6133
0.6	0.6661	0.6659	0.6659	0.6659
0.7	0.7319	0.7319	0.7320	0.7320
0.8	0.8107	0.8110	0.8110	0.8110
0.9	0.9016	0.9011	0.9012	0.9012
1.0	1.0000	1.0000	1.0000	1.0000

for the case ($T_0 = 0.5$; $N_c = 0.6$; $H = 0.0$). Clearly, as the boundary is approached (x = 0.8 and 0.9), the convergence rate decreases, though only slightly, as expected from utilizing the inversion formula. Again, the overall performance is quite consistent, and an excellent agreement was found with the numerical results obtained through subroutine DMOLCH/IMSL [29].

Nonlinear convection–diffusion (transient problem) [19]

The hybrid solution for problems with nonlinear convective terms is now illustrated through consideration of the one-dimensional nonlinear Burgers equation [19], which is a frequently employed model equation for transient convection–diffusion phenomena, and used for development and validation of numerical schemes. The mathematical formulation of the problem here considered is:

$$\frac{\partial T(x,t)}{\partial t} + u(T)\frac{\partial T(x,t)}{\partial x} = \nu \frac{\partial^2 T(x,t)}{\partial x^2}, \quad 0 < x < 1, \quad t > 0 \tag{9a}$$

with initial and boundary conditions given, respectively, by

$$T(x,0) = 1, \quad 0 \leqslant x \leqslant 1 \tag{9b}$$

$$T(0,t) = 1; \quad T(1,t) = 0, \quad t > 0 \tag{9c,d}$$

and for the present application the nonlinear function $u(T)$ is taken as

$$u(T) = u_0 + bT. \tag{9e}$$

Numerical results were obtained for typical values of the parameters that govern the relative importance of convection (linear and nonlinear terms) and diffusion, u_0, b, and ν. Truncated systems of order $N \leqslant 30$ were solved through IMSL subroutine DIVPAG, with sufficient accuracy requirement in terms of relative error, in order to demonstrate the convergence characteristics of the hybrid solution. Table 2 presents the potential distributions, at different values of $t = 0.1$ and 0.5, for increasing values of N. The excellent convergence behavior is easily noticeable throughout Table 2, but it is interesting to note the behavior with respect to the governing parameters. As usual in eigenfunction expansion techniques, convergence becomes slower for decreasing t; also, as the importance of convection increases, either through the linear (u_0) or nonlinear (b) contributions, larger systems are required to provide the same relative accuracy. For instance, with $b = 0.01$ and $u_0 = 1.0$, convergence to five digits is achieved with $N \simeq 15$, with $b = 0.5$ and $u_0 = 1.0$, 15–20 terms are required, while for $b = 5.0$ and $u_0 = 1.0$ convergence is reached for $N \simeq 25$. For validation purposes, a semi-discrete scheme based on the combined use of spatial collocation and the method of lines was employed, which is readily available in subroutine DMOLCH from the IMSL library [29], for one-dimensional parabolic problems. The results from this well-established routine are in excellent agreement with those here presented, for 31 grid points in the spatial discretization.

Table 2. Nonlinear Burgers equation: convergence of hybrid solution and comparison with numerical solution

N	5	10	15	20	30	Numerical†
x	$t = 0.1$ ($u_0 = 1.0$; $b = 0.01$; $\nu = 1.0$)					
0.1	0.98152	0.98108	0.98111	0.98113	0.98112	0.98111
0.3	0.92128	0.92131	0.92132	0.92132	0.92132	0.92126
0.5	0.79882	0.79863	0.79861	0.79861	0.79861	0.79853
0.7	0.57169	0.57254	0.57250	0.57249	0.57250	0.57241
0.9	0.22014	0.22054	0.22047	0.22043	0.22045	0.22041
x	$t = 0.5$ ($u_0 = 1.0$; $b = 0.01$; $\nu = 1.0$)					
0.1	0.93980	0.93979	0.93979	0.93979	0.93979	0.93979
0.3	0.79919	0.79919	0.79119	0.79919	0.79919	0.79919
0.5	0.62622	0.62621	0.62621	0.62621	0.62621	0.62621
0.7	0.41335	0.41334	0.41334	0.41334	0.41334	0.41334
0.9	0.15194	0.15194	0.15194	0.15194	0.15194	0.15194
x	$t = 0.1$ ($u_0 = 1.0$; $b = 0.5$; $\nu = 1.0$)					
0.1	0.98507	0.98458	0.98461	0.98463	0.98462	0.98461
0.3	0.93240	0.93243	0.93244	0.93243	0.93243	0.93238
0.5	0.81800	0.81774	0.81772	0.81772	0.81772	0.81764
0.7	0.59425	0.59409	0.59404	0.59403	0.59403	0.59395
0.9	0.23064	0.23110	0.23100	0.23097	0.23099	0.23095
x	$t = 0.5$ ($u_0 = 1.0$; $b = 0.5$; $\nu = 1.0$)					
0.1	0.95031	0.95034	0.95032	0.95032	0.95032	0.95032
0.3	0.82591	0.82594	0.82594	0.82593	0.82593	0.82593
0.5	0.66018	0.66014	0.66014	0.66014	0.66014	0.66014
0.7	0.44271	0.44274	0.44273	0.44273	0.44273	0.44273
0.9	0.16424	0.16431	0.16429	0.16428	0.16429	0.16429
x	$t = 0.1$ ($u_0 = 1.0$; $b = 5.0$; $\nu = 1.0$)					
0.1	1.0004	0.99846	0.99849	0.99852	0.99851	0.99851
0.3	0.98887	0.98897	0.98900	0.98897	0.98897	0.98896
0.5	0.94953	0.94774	0.94771	0.94770	0.94771	0.94769
0.7	0.79457	0.79337	0.79330	0.79325	0.79328	0.79324
0.9	0.35350	0.35452	0.35430	0.35420	0.35426	0.35423
x	$t = 0.5$ ($u_0 = 1.0$; $b = 5.0$; $\nu = 1.0$)					
0.1	0.99799	0.99653	0.99655	0.99658	0.99657	0.99657
0.3	0.97866	0.97903	0.97904	0.97901	0.97901	0.97901
0.5	0.92319	0.92232	0.92226	0.92226	0.92227	0.92226
0.7	0.75150	0.75122	0.75111	0.75108	0.75110	0.75109
0.9	0.32549	0.32671	0.32649	0.32641	0.32646	0.32645

† Subroutine DMOLCH/IMSL [29] (31 grid points).

Nonlinear equation coefficients (diffusion problem) [10]

We consider heat conduction in a finite slab with a temperature dependent thermal conductivity, given in dimensionless form as:

$$\frac{\partial T(x,t)}{\partial t} = \frac{\partial}{\partial x}\left[K(T)\frac{\partial T(x,t)}{\partial x}\right], \quad 0 < x < 1, \quad t > 0 \tag{10a}$$

and initial and boundary conditions

$$T(x,0) = 1, \quad 0 \leqslant x \leqslant 1 \tag{10b}$$

$$\frac{\partial T(0,t)}{\partial x} = 0; \quad T(1,t) = 0, \quad t > 0 \tag{10c,d}$$

and $K(T)$ in the present application is taken as

$$K(T) = 1 + bT. \tag{10e}$$

The application considered was solved for different values of parameter b in the thermal conductivity expression, equation (10e), namely, $b = 0.1$, 1.0 and 5.0, in order to illustrate the effect of an increasing nonlinearity on the convergence behavior of the proposed hybrid solution. Table 3 shows numerical results for the temperature distribution within the slab at different times, $t = 0.1$ and 0.5. The ODE system was solved for increasing truncation orders up to $N = 30$, allowing for an inspection of convergence characteristics. As expected, for this eigenfunction expansion technique, a larger number of terms is required for decreasing values of t. Also, as b increases, and especially for shorter times, fully converged results to five digits may require larger truncation orders. For $b = 5.0$ and $t = 0.1$, the numerical results shown for $N = 30$ are converged to the fourth digit, while for $t = 0.5$ are correct for all five digits provided. Therefore, although some influence of the parameter b was observed, it can be said that the present approach is capable of handling strong nonlinear influence with basically the same performance. It is clearly noticeable that three or even four digits of precision are attainable at the lower values of N in all situations considered, with significant savings in cost with respect to higher orders. The last column illustrates the excellent agreement with a well-established routine for one-dimensional parabolic problems available in the IMSL package [29], which uses the semi-discrete method of lines combined to a collocation scheme with cubic hermite polynomials.

Table 3. Heat conduction with variable thermal conductivity: convergence behavior of hybrid solution and comparison with numerical approach

N	5	10	15	20	30	Numerical†
x			$t = 0.1$ ($b = 0.1$)			
0.1	0.93104	0.93105	0.93104	0.93104	0.93104	0.93097
0.3	0.86765	0.86765	0.86763	0.86763	0.86763	0.86754
0.5	0.72686	0.72692	0.72690	0.72690	0.72690	0.72680
0.7	0.49505	0.49499	0.49497	0.49497	0.49497	0.49488
0.9	0.17826	0.17854	0.17850	0.17849	0.17850	0.17846
x			$t = 0.5$ ($b = 0.1$)			
0.1	0.35182	0.35182	0.35182	0.35182	0.35182	0.35178
0.3	0.31809	0.31809	0.31809	0.31809	0.31809	0.31805
0.5	0.25348	0.25349	0.25348	0.25348	0.25348	0.25346
0.7	0.16366	0.16365	0.16365	0.16365	0.16365	0.16363
0.9	0.05671	0.05674	0.05674	0.05673	0.05674	0.05673
x			$t = 0.1$ ($b = 1.0$)			
0.1	0.83759	0.83775	0.83764	0.83763	0.83764	0.83757
0.3	0.78110	0.78105	0.78093	0.78092	0.78094	0.78086
0.5	0.66185	0.66242	0.66228	0.66225	0.66228	0.66220
0.7	0.47166	0.47102	0.47076	0.47079	0.47080	0.47073
0.9	0.18441	0.18780	0.18745	0.18725	0.18736	0.18731
x			$t = 0.5$ ($b = 1.0$)			
0.1	0.26141	0.26143	0.26142	0.26142	0.26142	0.26140
0.3	0.23896	0.23896	0.23895	0.23895	0.23895	0.23893
0.5	0.19453	0.19457	0.19456	0.19456	0.19456	0.19455
0.7	0.12964	0.12960	0.12959	0.12959	0.12959	0.12958
0.9	0.04654	0.04673	0.04671	0.04670	0.04670	0.04670
x			$t = 0.1$ ($b = 5.0$)			
0.1	0.58117	0.58168	0.58133	0.58127	0.58135	0.58140
0.3	0.54812	0.54813	0.54771	0.54767	0.54775	0.54780
0.5	0.47637	0.47791	0.47744	0.47731	0.47743	0.47746
0.7	0.36362	0.36214	0.36123	0.36121	0.36140	0.36140
0.9	0.16105	0.17199	0.17082	0.16981	0.17035	0.17024
x			$t = 0.5$ ($b = 5.0$)			
0.1	0.12374	0.12377	0.12376	0.12376	0.12376	0.12377
0.3	0.11431	0.11432	0.11431	0.11431	0.11431	0.11432
0.5	0.09511	0.09518	0.09516	0.09516	0.09516	0.09517
0.7	0.06583	0.06578	0.06576	0.06576	0.06576	0.06577
0.9	0.02483	0.02513	0.02510	0.02508	0.02509	0.02509

† Subroutine DMOLCH/IMSL LIBRARY [29] (31 grid points).

Boundary layer equations [24]

In this section we illustrate the analysis of the boundary layer equations for simultaneous heat and fluid flow inside ducts. The momentum and energy equations are transformed concurrently, based on specific auxiliary eigenvalue problems. We consider hydrodynamically and thermally developing incompressible laminar flow of a Newtonian fluid, between parallel-plates subjected to a uniform wall temperature and uniform inlet conditions, for both velocity and temperature fields. Physical properties are assumed constant and viscous dissipation and free convection effects are considered negligible, although not a limitation for application of the present approach. Within the range of validity for the boundary layer hypothesis, the problem formulation in dimensionless form is written as:

Continuity:

$$\frac{\partial U(R,Z)}{\partial Z} + \frac{\partial V(R,Z)}{\partial R} = 0, \quad 0 < R < 1, \quad Z > 0 \tag{11a}$$

Z-momentum equation:

$$U\frac{\partial U(R,Z)}{\partial Z} + V\frac{\partial U(R,Z)}{\partial R} = -\frac{\mathrm{d}p^*}{\mathrm{d}Z} + \frac{1}{Re}\frac{\partial^2 U}{\partial R^2}, \quad 0 < R < 1, \quad Z > 0 \tag{11b}$$

Table 4. Boundary layer equations: convergence analysis of duct centerline velocity and validation of adaptive procedure (Tol. = 10^{-5})

N / X^+	5	10	15	20	25	30	Adapt.	N	Ref. [30]
0.375	1.1101	1.1190	1.1221	1.1232	1.1239	1.1242	1.1242	30	1.124
0.5	1.1271	1.1386	1.1413	1.1422	1.1427	1.1430	1.1430	30	1.144
1.0	1.1904	1.1979	1.1994	1.1999	1.2001	1.2002	1.2002	29	1.203
1.5	1.2380	1.2423	1.2432	1.2435	1.2435	1.2435	1.2435	28	1.246
2.0	1.2764	1.2690	1.2797	1.2797	1.2796	1.2796	1.2796	28	1.282
2.5	1.3092	1.3108	1.3110	1.3108	1.3107	1.3107	1.3107	28	1.312
5.0	1.4148	1.4139	1.4133	1.4129	1.4126	1.4126	1.4126	26	1.411
12.5	1.4921	1.4917	1.4914	1.4913	1.4913	1.4913	1.4913	14	1.490

Energy equation:

$$U\frac{\partial\theta(R,Z)}{\partial Z}+V\frac{\partial\theta(R,Z)}{\partial R}=\frac{1}{Pe}\frac{\partial^2\theta}{\partial R^2},$$

$$0<R<1,\quad Z>0 \tag{11c}$$

with inlet and boundary conditions given, respectively, by

$$U(R,0)=1;\quad V(R,0)=0;\quad \theta(R,0)=1 \tag{11d–f}$$

$$\frac{\partial U(0,Z)}{\partial R}=0;\quad V(0,Z)=0;\quad \frac{\partial\theta(0,Z)}{\partial R}=0 \tag{11g–i}$$

$$U(1,Z)=0;\quad V(1,Z)=0;\quad \theta(1,Z)=0. \tag{11j–l}$$

First of all, the adaptive procedure is validated, and the convergence behavior illustrated, for the velocity problem under separation of the fully developed solutions. Table 4 presents results for the duct centerline velocity along the dimensionless axial coordinate, for different values of the truncation order in the velocity field expansion, from $N = 5$ up to 30. Also shown are the final results achieved through implementation of the adaptive procedure, and the automatically controlled values of the system size N. Clearly, as expected, the adaptive scheme results reproduce the fully converged solutions to within the user prescribed accuracy requirements, in this case a relative error target of 10^{-5}. The results from the purely numerical approach in ref. [30] are also validated, demonstrating a very good agreement with the error controlled results of the present approach.

Figure 1 illustrates the automatic reduction on the ODEs systems sizes, for both the velocity and temperature fields, achieved through implementation of the adaptive procedure along the integration path in Z. The temperature field is still more rapidly converging than the velocity expansion, even after separation of the fully developed flow solution. The computation represented in Fig. 1 was observed to be 23 times faster than the numerical integration of the ODE systems with a fixed number of equations, i.e. $N = M = 40$, which reconfirms the marked advantages in the implementation of the adaptive procedure.

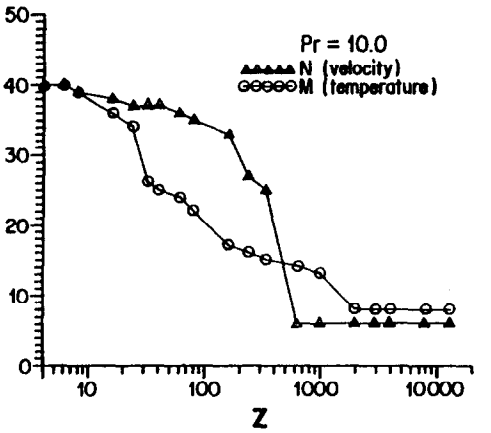

FIG. 1. Automatic reduction of the truncated ODEs systems sizes along integration path, through adaptive procedure (error target = 10^{-5}).

Nonlinear convection–diffusion (steady-state) [20]

The integral transform approach is now employed in the analysis of the two-dimensional steady Burgers equation. This important test case represents a model equation for the competition of convection and diffusion phenomena in multidimensional steady situations. The problem formulation was selected since an exact solution for the linearized version of this problem is readily obtainable, that can be useful for validation purposes. The partial differential system is then given by:

$$\frac{\partial^2 T(x,y)}{\partial y^2}+\frac{\partial^2 T(x,y)}{\partial x^2}=u\frac{\partial T(x,y)}{\partial x}+v\frac{\partial T(x,y)}{\partial y},$$

$$0<x<1,\quad 0<y<1 \tag{12a}$$

with boundary conditions

$$T(x,0)=\frac{1-\exp[u_0(x-1)]}{1-\exp[-u_0]};$$

$$T(x,1)=0,\quad 0\leqslant x\leqslant 1 \tag{12b,c}$$

$$T(0,y)=\frac{1-\exp[u_0(y-1)]}{1-\exp[-u_0]};$$

$$T(1,y)=0,\quad 0\leqslant y\leqslant 1. \tag{12d,e}$$

Table 5. Steady Burgers equation: convergence of potential $T(x, y)$ at different positions (x, y), for $u = v = u_0$ (linear problem—Tol = 10^{-4})

	$u_0 = 1.0$								
N	$x = 0.1$ $y = 0.1$	$x = 0.5$ $y = 0.1$	$x = 0.9$ $y = 0.1$	$x = 0.1$ $y = 0.5$	$x = 0.5$ $y = 0.5$	$x = 0.9$ $y = 0.5$	$x = 0.1$ $y = 0.9$	$x = 0.5$ $y = 0.9$	$x = 0.9$ $y = 0.9$
4	0.8803	0.5836	0.1398	0.5836	0.3869	0.0928	0.1412	0.0934	0.0244
6	0.8811	0.5846	0.1411	0.5842	0.3876	0.0936	0.1413	0.0938	0.0226
8	0.8813	0.5842	0.1415	0.5844	0.3874	0.0938	0.1413	0.0937	0.0227
10	0.8814	0.5844	0.1415	0.5844	0.3875	0.0938	0.1413	0.0937	0.0227
12	0.8814	0.5843	0.1415	0.5844	0.3874	0.0938	0.1413	0.0937	0.0227
Anal.	0.8813	0.5844	0.1413	0.5844	0.3875	0.0937	0.1413	0.0937	0.0227

Problem (12) was computationally solved for both the linearized ($u = v = u_0$) and nonlinear ($u = v = u_0 T$) versions, with the use of subroutine DBVPFD from the IMSL library to evaluate the transformed ODE system. A truncation order of $N \leqslant 18$ was employed throughout, with a relative error target of 10^{-4}, which was more than sufficient to provide convergence within the full range of parameters investigated. In order to illustrate the automatic accuracy control feature, we present in Table 5 a comparison of the present results for the linearized problem with the exact solution, at different positions x, y within the domain. The fully converged results, for the case of $u_0 = 1$ presented, are in agreement to within ± 1 in the last digit given, when compared to the exact solution, as expected from an automatic accuracy control scheme with a relative error target of 10^{-4}.

The convergence behavior of the eigenfunction expansions for the nonlinear problem is now illustrated for different values of the parameter u_0, which governs the relative importance of convection and diffusion effects. The parameter u_0 was varied in the range of 0.1, 1.0 and 10, to cover the three possibilities of the convection–diffusion ratio.

Tables 6–8 show, respectively, the convergence behavior for $u_0 = 0.1$, 1.0 and 10, at different representative positions within the domain. It can be clearly observed that for increasing importance of the convection effect, the convergence rates decrease somehow, although not markedly enough to inhibit a fully converged solution within practical limits. For instance, at $u_0 = 0.1$ even the results for $N = 4$ are within ± 1 in the last digit of the converged solution; at $u_0 = 1$, some results are converged for $N = 4$ while others require $N = 6$ or 8; at $u_0 = 10$, when convection becomes more important, convergence is achieved with $N = 8$ in the most favorable position and with $N = 12$ or 14 where the convective effects are more pronounced. The explanation for this behavior is immediate, since the convection terms play the role of a source term for the 'diffusion' problem solved through the eigenfunction expansion approach. Such expansions experience a reduction of convergence speed due to the presence of nonhomogeneous terms in addition to the diffusion operators. However, when the source term effect is sufficiently important to impede convergence within a reasonable limit, a few different alternatives have already been developed in order to enhance the convergence rates, such as the integral balance approach and filtering solutions presented in ref. [5], for both parabolic and elliptic diffusion problems. For the present application, in the extreme situations of $u_0 \gg 10$, such an alternative enhanced series is recommended. In addition, auxiliary problems which include some information about the convection, even through linearized coefficients, may offer some advantages.

Natural convection in a porous cavity [25]

We consider two-dimensional, steady natural convection in a saturated porous rectangular enclosure, subjected to uniform internal heat generation and to cooling at both side walls, which are kept at the same uniform temperature. The top and bottom ends are kept insulated. Within the validity of Darcy's law,

Table 6. Steady Burgers equation: convergence of potential $T(x, y)$ at different positions (x, y), for $u = v = u_0 T$ (nonlinear problem)

	$u_0 = 0.1$								
N	$x = 0.1$ $y = 0.1$	$x = 0.5$ $y = 0.1$	$x = 0.9$ $y = 0.1$	$x = 0.1$ $y = 0.5$	$x = 0.5$ $y = 0.5$	$x = 0.9$ $y = 0.5$	$x = 0.1$ $y = 0.9$	$x = 0.5$ $y = 0.9$	$x = 0.9$ $y = 0.9$
4	0.8172	0.4614	0.0934	0.4614	0.2573	0.0516	0.0935	0.0517	0.0104
6	0.8173	0.4614	0.0935	0.4614	0.2573	0.0516	0.0935	0.0516	0.0103
8	0.8173	0.4614	0.0935	0.4614	0.2573	0.0516	0.0935	0.0516	0.0103
10	0.8173	0.4614	0.0935	0.4614	0.2573	0.0516	0.0935	0.0516	0.0103
12	0.8173	0.4614	0.0935	0.4614	0.2573	0.0516	0.0935	0.0516	0.0103

Table 7. Steady Burgers equation: convergence of potential $T(x, y)$ at different positions (x, y), for $u = v = u_0 T$ (nonlinear problem)

	$u_0 = 1.0$								
N	$x = 0.1$ $y = 0.1$	$x = 0.5$ $y = 0.1$	$x = 0.9$ $y = 0.1$	$x = 0.1$ $y = 0.5$	$x = 0.5$ $y = 0.5$	$x = 0.9$ $y = 0.5$	$x = 0.1$ $y = 0.9$	$x = 0.5$ $y = 0.9$	$x = 0.9$ $y = 0.9$
4	0.8762	0.5657	0.1280	0.5660	0.3314	0.0687	0.1293	0.0690	0.0104
6	0.8767	0.5661	0.1284	0.5660	0.3314	0.0687	0.1286	0.0685	0.0139
8	0.8768	0.5660	0.1284	0.5660	0.3314	0.0687	0.1284	0.0687	0.0138
10	0.8768	0.5660	0.1285	0.5660	0.3314	0.0687	0.1284	0.0686	0.0138
12	0.8768	0.5660	0.1285	0.5660	0.3314	0.0687	0.1284	0.0687	0.0138

Table 8. Steady Burgers equation: convergence of potential $T(x, y)$ at different positions (x, y), for $u = v = u_0 T$ (nonlinear problem)

	$u_0 = 10.0$								
N	$x = 0.1$ $y = 0.1$	$x = 0.5$ $y = 0.1$	$x = 0.9$ $y = 0.1$	$x = 0.1$ $y = 0.5$	$x = 0.5$ $y = 0.5$	$x = 0.9$ $y = 0.5$	$x = 0.1$ $y = 0.9$	$x = 0.5$ $y = 0.9$	$x = 0.9$ $y = 0.9$
4	0.9777	0.9762	0.5220	0.9780	0.9681	0.4504	0.5571	0.4608	0.1592
6	0.9946	0.9965	0.5467	0.9910	0.9795	0.4602	0.5514	0.4595	0.1576
8	0.9990	0.9918	0.5503	0.9926	0.9789	0.4611	0.5494	0.4617	0.1569
10	0.9998	0.9930	0.5502	0.9928	0.9790	0.4611	0.5490	0.4609	0.1567
12	0.9999	0.9927	0.5499	0.9928	0.9790	0.4611	0.5492	0.4613	0.1567
14	0.9999	0.9928	0.5498	0.9928	0.9790	0.4611	0.5496	0.4611	0.1567
16	0.9999	0.9928	0.5498	0.9928	0.9790	0.4611	0.5498	0.4612	0.1568

and after invoking the Boussinesq approximation, the problem formulation in dimensionless form is given by [25]:

$$\frac{\partial^2 \psi(x,y)}{\partial y^2} + \frac{\partial^2 \psi(x,y)}{\partial x^2} = -R\frac{\partial T(x,y)}{\partial x} \tag{13a}$$

$$\frac{\partial^2 T(x,y)}{\partial y^2} + \frac{\partial^2 T(x,y)}{\partial x^2} + 1 = \frac{\partial \psi}{\partial y}\frac{\partial T}{\partial x} - \frac{\partial \psi}{\partial x}\frac{\partial T}{\partial y},$$

$$\text{in } 0 < x < 1, \quad 0 < y < A \tag{13b}$$

with boundary conditions

$$\psi(0,y) = \psi(1,y) = 0; \quad T(0,y) = T(1,y) = 0 \tag{13c–f}$$

$$\psi(x,0) = \psi(x,A) = 0; \quad \frac{\partial T(x,0)}{\partial y} = \frac{\partial T(x,A)}{\partial y} = 0 \tag{13g–j}$$

and the dimensionless Darcy velocities are obtained from the stream function distribution according to the definitions

$$u = \frac{\partial \psi}{\partial y}; \quad v = -\frac{\partial \psi}{\partial x}. \tag{14a,b}$$

The present problem was solved for different values of the governing parameters, Rayleigh number and aspect ratio, namely, $A = 2$ and 5, $R = 10$, 50, 100, 500, and 1000.

First, the convergence behavior of this eigenfunction expansion-type approach is illustrated in Tables 9 and 10, for stream function and temperature, respectively, with $R = 100$ and $A = 5$. To simplify the tables, the truncation orders in the two expansions were kept equal, i.e. $N = M$, and varying from $M = 5$ up to 22. The ODE solver was employed with a required tolerance of 10^{-4}, which means that the fully converged results are expected to be correct to ± 1 in the fourth significant digit. The Tables present results for ψ and T at various locations within the cavity, in order to cover all the regions of different physical and mathematical behavior. From inspection of Table 9 it can be noticed that the temperature results for $N = 9$ are, in general, already fully converged to the four digits required, with a slightly slower convergence rate close to the wall at $x = 0$, within the boundary layer.

From Table 10, the stream function results are shown to be essentially fully converged for $N = 13$, again with some slight improvement in convergence for the more internal points in the horizontal direction. Similar conclusions concerning this well-behaved convergence were drawn for the other cases tested, with almost uniform rates within the medium.

The fully converged integral transform results validate finite difference results in all situations considered [31], both in the interior of the enclosure and in the vicinity of the top and bottom end walls, where the variables experience more significant variations. These results were obtained with $N = M \leqslant 22$, and a relative error target for the boundary value problem solver of 10^{-4}. A typical run in the VAX 8810 computer took about 138 s of CPU time.

Navier–Stokes equations [26, 27]

The next natural step in the demonstration of the present hybrid approach is the solution of the

Table 9. Natural convection in porous enclosure: convergence of temperature distribution ($N = M$; Tol = 10^{-4}; $R = 100$; $A = 5$)

		x				
y	N	0.1	0.2	0.3	0.4	0.5
	5	0.03210	0.05924	0.08182	0.09713	0.1028
	9	0.03200	0.05931	0.08179	0.09719	0.1028
0.0	13	0.03202	0.05932	0.08178	0.09718	0.1027
	17	0.03202	0.05932	0.08178	0.09718	0.1027
	22	0.03202	0.05932	0.08179	0.09719	0.1027
	5	0.03390	0.06136	0.08355	0.09820	0.1036
	9	0.03378	0.06145	0.08350	0.09828	0.1035
0.1111	13	0.03379	0.06146	0.08350	0.09827	0.1035
	17	0.03380	0.06145	0.08350	0.09827	0.1035
	22	0.03379	0.06145	0.08350	0.09827	0.1035
	5	0.04493	0.07953	0.1046	0.1193	0.1244
	9	0.04479	0.07962	0.1045	0.1194	0.1244
2.2222	13	0.04480	0.07963	0.1045	0.1194	0.1244
	17	0.04481	0.07963	0.1045	0.1194	0.1244
	22	0.04480	0.07963	0.1045	0.1194	0.1244
	5	0.06142	0.1025	0.1271	0.1397	0.1438
	9	0.06124	0.1026	0.1270	0.1398	0.1437
4.8889	13	0.06126	0.1026	0.1270	0.1397	0.1437
	17	0.06126	0.1026	0.1270	0.1397	0.1437
	22	0.06126	0.1026	0.1270	0.1397	0.1437
	5	0.06583	0.1063	0.1299	0.1415	0.1454
	9	0.06553	0.1065	0.1297	0.1416	0.1453
5.0000	13	0.06556	0.1065	0.1297	0.1416	0.1453
	17	0.06556	0.1065	0.1297	0.1416	0.1453
	22	0.06556	0.1065	0.1297	0.1416	0.1453

Table 10. Natural convection in porous enclosure: convergence of stream function distribution ($N = M$; Tol = 10^{-4}; $R = 100$; $A = 5$)

		x				
y	N	0.1	0.2	0.3	0.4	0.5
	5	0.2790	0.3424	0.2969	0.1673	0.0
	9	0.2736	0.3446	0.2951	0.1678	0.0
0.0	13	0.2744	0.3451	0.2952	0.1681	0.0
	17	0.2743	0.3451	0.2953	0.1679	0.0
	22	0.2743	0.3450	0.2953	0.1679	0.0
	5	0.5823	0.7634	0.6719	0.3814	0.0
	9	0.5752	0.7660	0.6693	0.3821	0.0
1.1111	13	0.5763	0.7666	0.6694	0.3824	0.0
	17	0.5762	0.7666	0.6696	0.3822	0.0
	22	0.5761	0.7666	0.6696	0.3822	0.0
	5	0.6030	0.7921	0.6981	0.3967	0.0
	9	0.5957	0.7948	0.6955	0.3974	0.0
2.2222	13	0.5969	0.7954	0.6956	0.3976	0.0
	17	0.5967	0.7954	0.6957	0.3974	0.0
	22	0.5966	0.7954	0.6957	0.3975	0.0
	5	0.6060	0.7964	0.7019	0.3989	0.0
	9	0.5987	0.7991	0.6993	0.3996	0.0
3.3333	13	0.5999	0.7997	0.6994	0.3999	0.0
	17	0.5997	0.7997	0.6996	0.3997	0.0
	22	0.5997	0.7996	0.6996	0.3997	0.0
	5	0.6177	0.8019	0.6995	0.3944	0.0
	9	0.6101	0.8048	0.6967	0.3952	0.0
4.4444	13	0.6113	0.8054	0.6968	0.3952	0.0
	17	0.6111	0.8054	0.6970	0.3952	0.0
	22	0.6111	0.8053	0.6970	0.3952	0.0

full Navier–Stokes equations. Therefore, the present application is aimed at advancing the integral transform method to handle this class of problems, here represented by the classical square cavity test case. The stream function-only formulation is preferred, since boundary conditions are explicitly provided and the auxiliary eigenvalue-type problem is more easily defined. The related nonlinear biharmonic partial differential equation is integral transformed by eliminating one of the space variables dependence, and obtaining an infinite system of coupled nonlinear ordinary differential equations for the transformed stream functions.

We consider two-dimensional steady incompressible laminar flow of a Newtonian fluid inside a square cavity, due to a top end wall continuously moving at a constant velocity. The related Navier–Stokes equations in vorticity–transport formulation and dimensionless form are written as:

$$\frac{1}{Re}\left[\frac{\partial^2\omega(x,y)}{\partial y^2}+\frac{\partial^2\omega(x,y)}{\partial x^2}\right]=\frac{\partial\psi}{\partial y}\frac{\partial\omega}{\partial x}-\frac{\partial\psi}{\partial x}\frac{\partial\omega}{\partial y} \tag{15a}$$

and,

$$\omega(x,y)=-\left[\frac{\partial^2\psi(x,y)}{\partial y^2}+\frac{\partial^2\psi(x,y)}{\partial x^2}\right],$$

$$\text{in } 0<x<1,\quad 0<y<1 \tag{15b}$$

where $\omega(x, y)$ is the vorticity, $\psi(x, y)$ is the stream function and Re is the Reynolds number. The appropriate boundary conditions are given by

$$\psi(0,y)=0;\quad \frac{\partial\psi(0,y)}{\partial x}=0,\qquad 0\leqslant y<1 \tag{15c,d}$$

$$\psi(1,y)=0;\quad \frac{\partial\psi(1,y)}{\partial x}=0,\qquad 0\leqslant y<1 \tag{15e,f}$$

$$\psi(x,0)=0;\quad \frac{\partial\psi(x,0)}{\partial y}=0,\qquad 0\leqslant x\leqslant 1 \tag{15g,h}$$

$$\psi(x,1)=0;\quad \frac{\partial\psi(x,1)}{\partial y}=-1,\quad 0<x<1. \tag{15i,j}$$

All the required boundary conditions are specified in terms of the stream function. Therefore, it becomes more convenient, especially when choosing the auxiliary eigenvalue-type problem, to rewrite equations (15a,b) in the so-called stream function-only formulation. Then, substituting equation (15b) into equation (15a), we find:

$$\frac{\partial^4\psi}{\partial x^4}+2\frac{\partial^4\psi}{\partial x^2\,\partial y^2}+\frac{\partial^4\psi}{\partial x^4}=\nabla^4\psi(x,y)$$

$$=Re\left[\frac{\partial\psi}{\partial y}\left(\frac{\partial^3\psi}{\partial x^3}+\frac{\partial^3\psi}{\partial y^2\,\partial x}\right)-\frac{\partial\psi}{\partial x}\left(\frac{\partial^3\psi}{\partial x^2\,\partial y}+\frac{\partial^3\psi}{\partial y^3}\right)\right]. \tag{16}$$

Equation (16) above together with boundary conditions (15c–j) form a nonlinear biharmonic-type prob-

lem, for which an exact solution is not attainable through the classical analytical solution methodologies.

The algorithm constructed is first of all employed to produce a set of benchmark results for the important special case of creeping flow ($Re = 0$) which is also used to validate the automatic global error control. A relative error target of 10^{-4} is adopted, and convergence is considered to be reached to within ± 1 in the fourth digit of the stream function. Table 11 below illustrates the convergence behavior of the stream function eigenfunction expansion for different positions within the cavity and increasing truncation orders N. The fully converged results are in excellent agreement with the exact solution, as expected from the global error control procedure. The recently reported results in ref. [32] are also considered for comparison purposes, which includes a semi-analytic solution and a finite elements implementation of the case $Re = 0$, both in excellent agreement.

Next, the convergence behavior of the present solutions with prescribed accuracy was investigated, by varying the number of terms retained in the eigenfunction expansions, N. Different values of Reynolds number were considered, which appear more frequently in the literature, for critical comparisons, namely, $Re = 0$, 100, 400 and 1000, with truncation orders $N \leqslant 21$. Fully converged results are, therefore, expected to be correct to within ± 1 in the fourth significant digit, for a relative error target of 10^{-4}.

Figures 2(a),(b) show the stream function profiles at the centerline of the cavity, $x = 0.5$, for the values of $Re = 100$ and 400, respectively, and different truncation orders, $N = 6$, 9, 12, 15, 18 and 21. Both graphs indicate that the curves are practically coincident for $N = 12$, 15, 18 and 21, with decreasing convergence rates for increasing Reynolds number, as expected, since the

Table 11. Convergence behavior of stream function expansion ($Re = 0$)

N	$x = 0.1$ $y = 0.1$	$x = 0.1$ $y = 0.5$	$x = 0.1$ $y = 0.9$
3	2.293E-4	7.587E-3	2.698E-2
4	2.141E-4	7.512E-3	2.991E-2
5	2.092E-4	7.485E-3	3.089E-2
6	2.082E-4	7.476E-3	3.101E-2
7	2.084E-4	7.472E-3	3.087E-2
8	2.088E-4	7.471E-3	3.073E-2
9	2.091E-4	7.470E-3	3.064E-2
10	2.092E-4	7.469E-3	3.059E-2
11	2.092E-4	7.469E-3	3.056E-2
N	$x = 0.5$ $y = 0.1$	$x = 0.5$ $y = 0.5$	$x = 0.5$ $y = 0.9$
3	3.081E-3	5.929E-2	7.424E-2
4	3.081E-3	5.913E-2	7.151E-2
5	3.071E-3	5.904E-2	7.266E-2
6	3.071E-3	5.900E-2	7.212E-2
7	3.069E-3	5.898E-2	7.235E-2
8	3.069E-3	5.896E-2	7.223E-2
9	3.069E-3	5.896E-2	7.229E-2
10	3.069E-3	5.896E-2	7.226E-2
11	3.069E-3	5.895E-2	7.227E-2

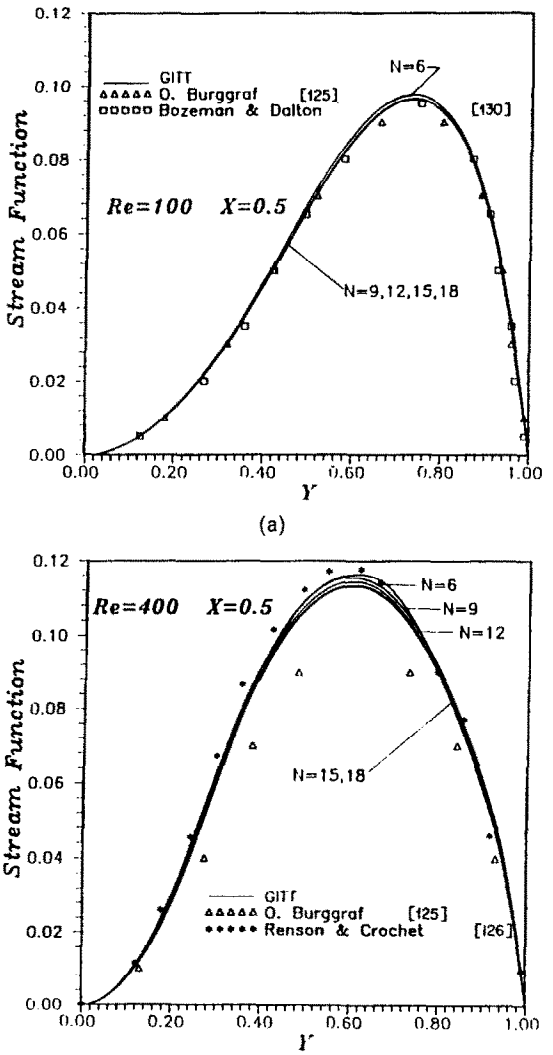

FIG. 2. (a) Convergence behavior of stream function ($x = 0.5$, $Re = 100$). (b) Convergence behavior of stream function ($x = 0.5$, $Re = 400$).

biharmonic equation becomes more non-homogeneous Also shown are some results from previously reported purely numerical approaches, for comparison purposes. Clearly, the early finite differences results of Burggraf [33] become increasingly inaccurate for higher Re, and even more recent contributions on finite elements with quadratic elements [34] are still reasonably inaccurate for moderate Reynolds numbers. The best agreement is achieved by efficient finite differences schemes, represented by the recent works of Ghia *et al.* [35] and Schreiber and Keller [36], as shown in the extensive comparisons in refs. [5, 27].

The same direct expansions here evaluated can be employed for higher Reynolds numbers, provided sufficiently large truncation orders are considered, and the price is paid in terms of increased storage and CPU time. Alternatively, one can extract information from the 'source function' represented by the con-

vection terms, making the nonhomogeneous part of the biharmonic-type equation less significant. This is accomplished by separating from the original potential a particular solution that includes the source terms, as proposed in ref. [5]. In addition, a different auxiliary problem may be considered, which accommodates some information on the increased importance of the convection terms as *Re* increases, for instance, through incorporation of linearized convective terms in the eigenvalue problem.

CLOSING REMARKS

The major advantages of the presented integral transform method are as follows.

(A) The hybrid numerical–analytical nature, characteristic of this approach, collapses most of the numerical effort into one single independent variable, i.e. the numerical integration of an ODE system, which is nowadays a very well-established task in numerical analysis, even for potentially stiff systems, including error control schemes.

(B) The wide availability of ODE solvers and other subroutines in scientific sub-routines packages, for intermediate computational tasks, makes the computational implementation of the present approach quite simple, based on successive calls to such easily accessible and simple to use routines.

(C) The automatic global error control and estimation offers the extremely attractive feature of working within an user prescribed accuracy and with an almost optimized computational effort, not frequently found in numerical methods for partial differential equations.

(D) Irregularly shaped domains, with respect to the coordinates system adopted, are directly handled either through description of the boundary surfaces in each coordinate in terms of the other spatial variables, or when required, by decomposing the domain in regularly shaped regions and analytically coupling these solutions for each subdomain.

(E) Due to the hybrid nature discussed above, the increase in computational effort is not too significant when the number of independent variables in the PDE system is increased. Therefore, one-, two- and three-dimensional applications are handled within the same order of magnitude of computer CPU time. Numerical experiments on the transient Burgers equation of the previous section confirmed this statement, with an increase of about 10% in CPU time for the two-dimensional case, and similarly for the three-dimensional situation. This is easily understood if one remembers that the numerical work in this approach is always reduced to a numerical integration of an ODE system (one single independent variable), while all the remaining independent variables are eliminated through integral transformation and recalled in analytic explicit form within the inversion formula, which is essentially a single, double or triple summation. This is indeed a major advantage over fully discrete approaches, which become in many cases prohibitive for multidimensional situations.

Future research needs are various and seem endless as more and more progress is achieved in this direction. The final objective will always be the establishment of automatic PDE solvers for general purposes, with minimum user intervention and expertise. Meanwhile, different classes of extensions to those base problems here presented are to be handled.

REFERENCES

1. A. V. Luikov, *Heat and Mass Transfer*. Mir Publishers, Moscow (1973).
2. M. N. Özisik, *Heat Conduction*. Wiley, New York (1980).
3. M. D. Mikhailov and M. N. Özisik, *Unified Analysis and Solutions of Heat and Mass Diffusion*. Wiley, New York (1984).
4. M. N. Özisik and R. L. Murray, On the solution of linear diffusion problems with variable boundary condition parameters, *J. Heat Transfer* **96C**, 48–51 (1974).
5. R. M. Cotta, *Integral Transforms in Computational Heat and Fluid Flow*. CRC Press, Boca Raton (1993).
6. R. M. Cotta, Computational integral transform approach in nonlinear diffusion and convection-diffusion problems, Laboratório di Ingegneria Nucleare di Montecuccolino, Serie Scientifica LIN-1202 (Invited Lecture), Universitá degli Studi di Bologna, Italy, July (1992).
7. R. M. Cotta and M. D. Mikhailov, The integral transform method, *Appl. Math. Modelling* **17**, 156–161 (1993).
8. M. D. Mikhailov and R. M. Cotta, Unified integral transform method, *J. Braz. Assoc. Mech. Sci.*, RBCM (Invited Paper), **12**(3), 301–310 (1990).
9. R. M. Cotta, Hybrid numerical analytical approach to nonlinear diffusion problems, *Num. Heat Transfer, Part B—Fundamentals* **17**, 217–226 (1990).
10. R. Serfaty and R. M. Cotta, Integral transform solutions of diffusion problems with nonlinear equation coefficients, *Int. Comm. Heat Mass Transfer* **17**, 852–864 (1990).
11. A. J. Diniz, J. B. Aparecido and R. M. Cotta, Heat conduction with ablation in a finite slab, *Int. J. Heat Technol.* **8**, 30–43 (1990).
12. N. J. Ruperti, Jr and R. M. Cotta, Heat conduction with ablation in multilayered media, *Proc. of the 11th Brazilian Congress of Mech. Eng.*, XI COBEM, pp. 413–416, São Paulo, Brazil, December (1991).
13. N. J. Ruperti, Jr, E. L. Zaparoli and R. M. Cotta, Hybrid solution for phase change problems in multiregion media, *30th Eurotherm Seminar–Heat Transfer in Phase Change Processes*, Orsay, France, October (1992).
14. J. W. Ribeiro and R. M. Cotta, Numerical-analytical study of nonlinear drying problems with radiative boundaries, *6th International Symposium on Transport Phenomena*, Seoul, Korea, pp. 209–214, May (1993).
15. R. M. Cotta and R. Ramos, Error analysis and improved formulations for extended surfaces, (Invited Lecture), *NATO Advanced Study Institute on Cooling of Electronic Systems*, Ismir, Turkey, June/July (1993).
16. J. W. Ribeiro and R. M. Cotta, On the solution of nonlinear drying problems in capillary porous media through integral transformation of Luikov equations, *Int. J. Num. Meth. Engng* (in press).
17. R. M. Cotta and R. Serfaty, Integral transform algorithm for parabolic diffusion problems with nonlinear

boundary and equation source terms, *Proc. of the 7th Int. Conf. on Num. Meth. for Thermal Problems*, Part 2, pp. 916–926, Stanford, CA, July (1991).
18. R. M. Cotta, R. Serfaty and R. O. C. Guedes, Integral transform solution of a class of transient convection–diffusion problems, *Proc. of the Int. Conf. on Advanced Computational Methods in Heat Transfer, Heat Transfer 90*, Vol. 1, pp. 239–250, Southampton, UK, July (1990).
19. R. Serfaty and R. M. Cotta, Hybrid analysis of transient nonlinear convection–diffusion problems, *Int. J. Num. Meth. Heat Fluid Flow* **2**, 55–62 (1992).
20. A. J. K. Leiroz and R. M. Cotta, On the solution of nonlinear elliptic convection–diffusion problems through the integral transform method, *Num. Heat Transfer, Part B—Fundamentals* **23**, 401–411, (1993).
21. M. D. Mikhailov and R. M. Cotta, Integral transform method for eigenvalue problems, *Comm. Num. Meth. Engng* (in press).
22. R. M. Cotta and T. M. B. Carvalho, Hybrid analysis of boundary layer equations for internal flow problems, *Proc. of the 7th Int. Conf. on Num. Meth. in Laminar and Turbulent Flow*, Part 1, pp. 106–115, Stanford, CA, July (1991).
23. T. M. B. Carvalho, R. M. Cotta and M. D. Mikhailov, Flow development in the entrance region of ducts, *Comm. Num. Meth. Engng* **9**, 503–509 (1993).
24. H. A. Machado and R. M. Cotta, Integral transform method for boundary layer equations in simultaneous heat and fluid flow problems, *Int. J. Num. Meth. Heat Fluid Flow* (in press).
25. C. Baohua and R. M. Cotta, Integral transform analysis of natural convection in porous enclosures, *Int. J. Num. Meth. Fluids* **17**, 1787–1801 (1993).
26. J. S. Perez Guerrero and R. M. Cotta, Integral transform method for Navier–Stokes equations in stream-function only formulation, *Int. J. Num. Meth. Fluids* **15**, 399–409 (1992).
27. R. M. Cotta, J. S. Perez Guerrero and F. Scofano Neto, Hybrid solution of the incompressible Navier–Stokes equations via integral transformation, *Proc. of the 2nd Int. Conf. Advanced Computational Methods in Heat Transfer, Heat Transfer 92*, Vol. 1, pp. 735–750, Milan, Italy, July (1992).
28. J. S. Perez Guerrero, R. M. Cotta and F. Scofano Neto, Integral transformation of Navier–Stokes equations for incompressible laminar flow in channels, *Proc. of the 8th Int. Conf. Num. Methods in Laminar & Turbulent Flow*, Vol. 2, pp. 1195–1206, Swansea, UK, July (1993).
29. IMSL Library, MATH/LIB, Houston, Texas (1987).
30. R. K. Shah and M. S. Bhatti, Laminar convective heat transfer in ducts. In *Handbook of Single-Phase Convective Heat Transfer* (Edited by S. Kakaç, R. K. Shah and W. Aung), (Chap. 3), pp. 3.1–3.137. Wiley, New York (1987).
31. M. Haajizadeh, A. F. Ozguç and C. L. Tien, Natural convection in a vertical porous enclosure with internal heat generation, *Int. J. Heat Mass Transfer* **27**, 1893–1902 (1984).
32. P. H. Gaskell, M. D. Savage and H. M. Thomson, Creeping flow—novel analytic and finite element solutions, *Proc. of the 7th Int. Conf. on Num. Meth. in Laminar & Turbulent Flow*, Part 2, pp. 1743–1753, Stanford, CA, July (1991).
33. O. R. Burggraf, Analytical and numerical studies of the structure of steady separated flows, *J. Fluid Mech.* **24**, 113–151 (1966).
34. A. Campion-Renson and M. J. Crochet, On the stream-function vorticity finite element solutions of Navier–Stokes equations, *Int. J. Num. Meth. Engng* **12**, 1809–1818 (1978).
35. U. Ghia, K. N. Ghia and C. T. Shin, High-*Re* solutions for incompressible flow using the Navier–Stokes equations and a multigrid method, *J. Comput. Phys.* **48**, 387–411 (1982).
36. R. Schreiber and H. B. Keller, Driven cavity flow by efficient numerical techniques, *J. Comput. Phys.* **49**, 310–333 (1983).